

The effect of fibre morphology on packing phenomena and bed properties in coalescers

Milica Hadnađev Kostić¹, Dunja Sokolović², Srđan Sokolović³, Thomas Laminger^{4,5} and Arpad Kiralj¹

¹University of Novi Sad, Faculty of Technology, Bul. Cara Lazara 1, Novi Sad, Serbia

²University of Novi Sad, Faculty of Technical Sciences, Trg Dositeja Obradovića 6, Novi Sad, Serbia

³NIS a.d. Novi Sad, Serbia, Narodnog fronta 12, Novi Sad, Serbia

⁴Vienna University of Technology, Institute of Chemical, Environmental and Bioscience Engineering, Austria TU WIEN, Getreidemarkt 9/166, A-1060 Vienna, Austria

⁵AGRANA Stärke GmbH - Werk Pischelsdorf, Industriegelände, 3435 Pischelsdorf, Austria

Abstract

In this study, fibre morphology of waste materials and its effect on packing phenomena and bed properties were investigated. Nine waste materials were used in bed coalescers. By scanning electron microscopy, it was determined that surfaces of all fibres were smooth, while cross-section differed from circular, rectangular to irregular. The fibres with circular cross-sections had diameters in the range of 12 ± 0.8 to 40 ± 4 μm , while the fibres of polypropylene bags and sponges appeared as strips with the widths of 452 ± 11 and 1001 ± 14 μm , respectively. It was also noticed that polyurethane fibres were connected forming a sponge-like structure, while polyethylene terephthalate fibres were interconnected at some points. In this work, experimental dependence of bed porosity on bed permeability was established for all investigated materials, which allows forming a fibre bed with desired permeability. The exception was the bed formed of fibres of polypropylene bags, which had the largest dimensions and yielded a different porosity-permeability dependence.

Keywords: bed permeability; bed porosity; fiber bed; coalescence filtration.

Available on-line at the Journal web address: <http://www.ache.org.rs/HI/>

TECHNICAL PAPER

UDC: 621.372.542-037.47+66.066.3:
539.217

Hem. Ind. 76(4) 197-208 (2022)

1. INTRODUCTION

Fibers are often used as a filter medium in bed coalescers for liquid-liquid or gas-liquid separation. The bed formed by fibres has an extremely complex structure in which complex phenomena occur due to the two-phase flow and different surface phenomena. Fibrous filter bed could exhibit high porosity up to 98 %. In the pores of the fibre bed, the dispersed phase is in the form of a capillary-conducted phase, droplets, and globules [1-3]. Depending on the physical properties, fibres are packed in a certain way, but most often as randomly packaged free fibres. It was indicated in literature that the fibre spatial arrangement significantly influences the position of droplets in the filter bed, which affects the coalescence efficiency [4]. The droplet position at fibre intersections is particularly significant. There are numerous studies on the effect of both physical and chemical properties of fibres on the dispersed phase collected in the bed, on its transport through the bed, as well as on attachment and detachment phenomena [5-11]. However, to the best of our knowledge, in the scientific literature, there is a lack of studies on the effect of fibre morphology on the bed geometry *i.e.*, bed permeability and bed porosity. Wetting properties and solid surface phenomena are governed by the surface chemical composition (determined by molecular structure), surface geometry, and topography as well as by the properties of the fluids [6-8,11-14]. Surface geometry can be considered as either local, such as surface roughness, or global, such as different shapes of the surface like spherical or cylindrical. For curved surfaces, such as granules or fibres, an adequate method for measuring the contact angle still does not exist. Four different surface topographies can be distinguished: smooth, micro-, nano-, and micro-nano structures [15-17].

Corresponding authors: Dunja Sokolović, University of Novi Sad, Faculty of Technical Sciences, Trg Dositeja Obradovića 6, 21000 Novi Sad, Serbia
E-mail: dunjaso@uns.ac.rs

Paper received: 22 December 2021; Paper accepted: 24 August; Paper published: 21 September 2022.

<https://doi.org/10.2298/HEMIND211224016K>



Based on the chemical nature, fibres can be classified as metal, ceramic, glass, and polymer fibres. It can be noted that these fibres drastically differ, not only regarding the chemical nature but also regarding flexibility as fibres could be rigid or elastic. Most of the polymer fibres are very elastic, while flexibility of metal fibres differs. Ceramic and glass fibres are considered completely rigid [9]. Most fibres used in bed coalescers are elastic, which enables bed packing at different bulk densities. Different bulk density alters the properties of the bed, such as bed permeability, bed porosity, and pore size [18-20].

Fibre dimensions and the cross-section shape are extremely important properties that directly affect the behaviour of droplets in the filter bed. Several authors have studied fibres with circular cross-sections and the influence of the fibre size on the efficiency of droplet separation from the continuous liquid or gaseous phase with contradictory conclusions [21-24]. Some authors argue that the increase in the fibre diameter decreases the separation efficiency, while others claim the opposite. However, it is generally agreed that the fibre diameter is an important parameter that influences the fluid flow through the bed, affecting separation of the dispersed phase from the fluid.

Our research group extensively investigated application of different waste fibre materials as filter media in bed coalescers used for the treatment of oily wastewater [25-28]. The investigated fibre materials showed high separation efficiency of mineral oil from water. In the previous research, it was noticed that the changes in bed permeability and bed porosity due to differences in pore size, volume and connectivity, directly affected the bed coalescence efficiency [19, 25].

The scope of this study was to investigate the fibre morphology of waste materials used in our previous studies and its effect on packing phenomena, bed permeability, and bed porosity.

2. MATERIALS AND METHODS

2. 1. Properties of investigated materials

Nine waste fibre materials were investigated in this research. Materials were obtained from local stores. Polyurethane material, PU, is waste generated during furniture manufacture as the excess parts from tailoring chairs and beds. Polypropylene, PP, is waste obtained from the manufacture of carpets. Polypropylene bag material, PPDJ, is waste from used vegetable bags. Polyethylene terephthalate, BA1, is waste produced from thermal filling used for winter clothes. Polyethylene terephthalate, PE, is waste attained from excess part of filters in kitchen aspirators. Stainless steel fibres with different diameters marked as SS40, SS20, and SS12 are the waste left after the production of steel wire. Stainless steel material, SSM is the waste metal sponge used for dishwashing.

Scanning electron microscopy (JEOL, JSM-6460 LV instrument, USA) and optical microscopy (Olympus BH.2 RFCA, Netherlands) were used for investigation of the fibre morphology (surface topography, fibre dimensions) and packing phenomena of waste fibre materials. The software ImageJ was applied for the measurement of fibre dimensions. At least three measurements were performed to determine the average fibre dimensions.

Density of fibre materials was measured by the weighing method, whereas the melting point was obtained by using a differential scanning calorimeter (Q20, TA Instruments, USA). Densities and melting points of investigated materials are given in Table 1.

Table 1. Properties of investigated materials

Material	Density, kg m ⁻³	Melting point, °C
Polyurethane (PU)	1200	309
Polypropylene (PP)	900	168
Polypropylene bag (PPDJ)	900	168
Polyethylene terephthalate (BA1)	1400	254
Polyethylene terephthalate (PE)	1400	250
Stainless steel (SS40)	7597	1510
Stainless steel (SS20)	7597	1510
Stainless steel (SS12)	7597	1510
Stainless steel sponge (SSM)	7597	1510

2. 2. Fibre beds

The experimental setup is presented in Figure 1. It consists of two Plexiglas tubes with 5 cm diameter and two piezometers. The first Plexiglas tube is 50 cm long and filled with the fibre material, *i.e.*, it represents the filter bed, while the second Plexiglas tube (1 m in length) is placed above it.

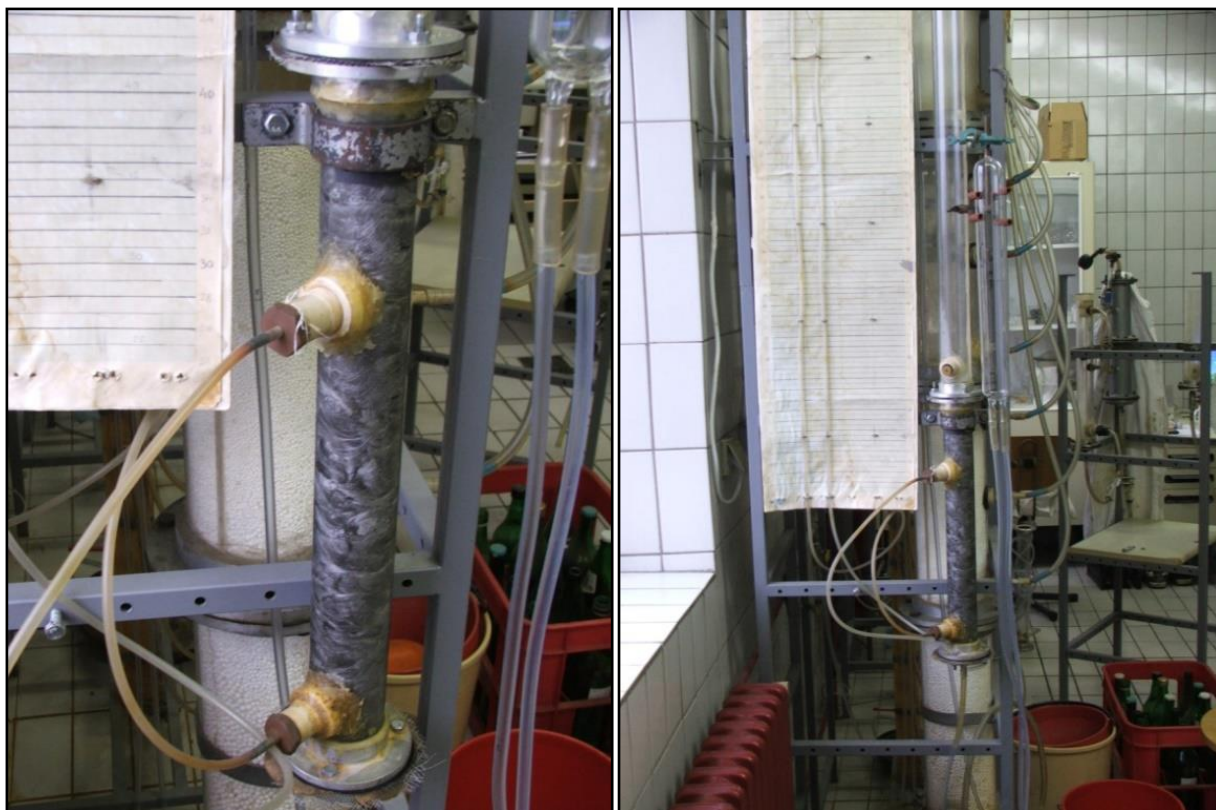


Figure 1. Experimental set up

Fibre materials applied in this research are flexible and therefore it was possible to form filter beds of different bulk densities, *i.e.* filter beds of different porosities.

The amount of fibre material, placed in the first Plexiglas tube, is determined based on the defined bed porosity. Mass of the material needed to form a filter bed of defined porosity is determined by the equation (1):

$$\varepsilon = 1 - \frac{\rho_B}{\rho} \quad (1)$$

For each new defined bed porosity, different amount of material was used, which is placed in the first Plexiglas tube. In order to ensure homogeneity of the filter bed, the measured fibre mass is divided into ten equal portions. The tube is then divided into ten segments of 5 cm in length, and filled with portions of the material, from the bottom to the top, segment by segment to ensure the bed homogeneity.

2. 3. Determination of bed porosity and bed permeability

Porosity is the fraction of empty spaces in a porous bed, *i.e.*, fraction of the void volume over the total bed volume. Fluid flows through a porous bed only through connected pores. The property of porous materials that indicates an available area for fluid flow, *i.e.*, the cross-sectional area available for fluid flow is called permeability [29].

Bed porosity was measured by the weighing method. The Darcy experiment was performed to determine the bed permeability for defined bed porosity.

The Darcy experiment was performed for different bed porosities, in the range from 83% to 98 % and for different fluid flowrates in the range from 30 to 600 cm³ min⁻¹.

The pressure drop across the bed during the flow of tap water was used to determine the bed permeability for the specific bed porosity based on the Darcy law. The experiments were repeated at least three times.

3. RESULTS AND DISCUSSION

3. 1. The effect of waste fibre morphology on packing phenomena in filter beds

Fibres of cheap and free available waste materials were investigated in this study with the aim to apply these waste fibres as filter media so to contribute to sustainable development and circular economy [28].

Fibre cross-section is one of the properties that could affect geometry of the resulting packed filter bed. Fibres could have circular, triangular, rectangular, square, or irregular cross-sections. Most of the fibres used in the present investigation have circular cross-sections, that is the PP, BA1, and PE fibres. The PPDJ and SSM fibres have rectangular cross-sections, while the SS fibres, have circular or irregular cross-sections, depending on the fibre thickness (Fig. 2).

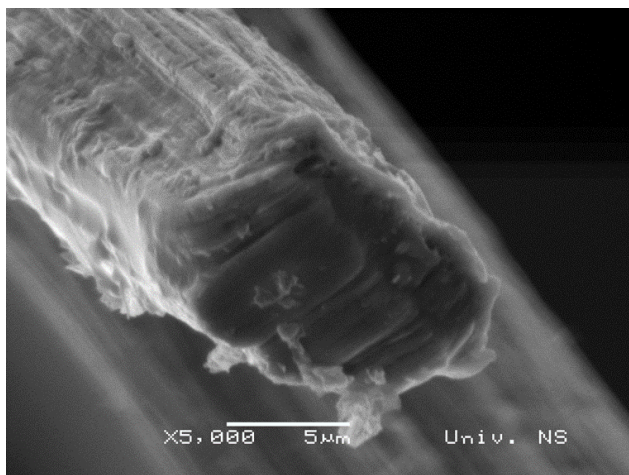


Figure 2. SEM image of the SS40 fibre cross-section (scale bar = 5 μm)

The SEM analysis has shown that most of the investigated fibres have a smooth or approximately smooth surfaces as in Figure 3 showing PU fibres clearly indicating extremely smooth surfaces and fibre interconnections. Similarly, PP fibres, exhibited smooth surfaces and uniform diameters (Fig. 4). In contrast, surfaces of stainless steel SS40 fibres are marginally wavy with slight longitudinal unevenness (Fig. 5). All other investigated materials exhibited also smooth surfaces.

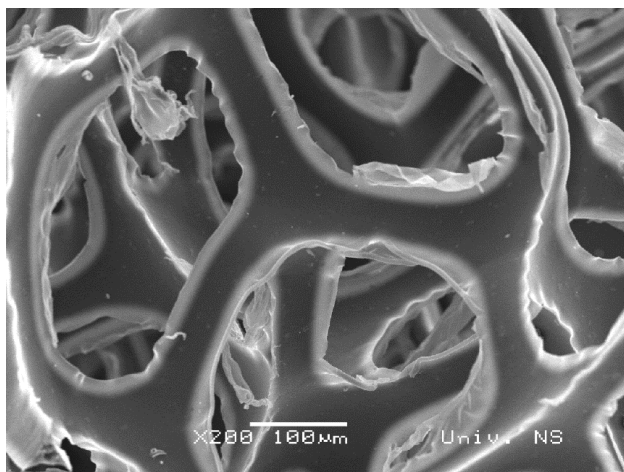


Figure 3. SEM micrograph of PU fibres (scale bar = 100 μm)

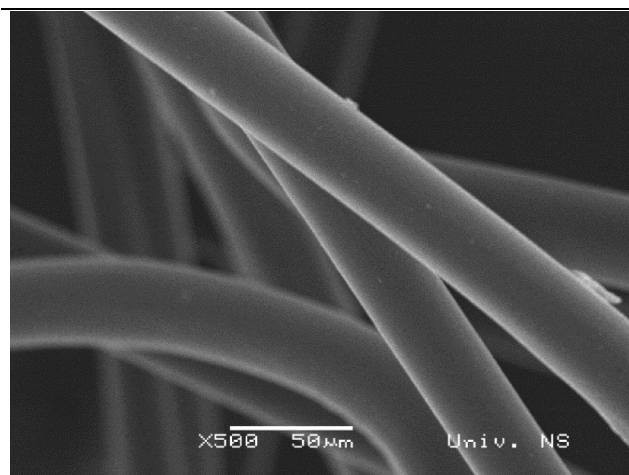


Figure 4. SEM micrographs of PP fibres (scale bar = 50 μm)

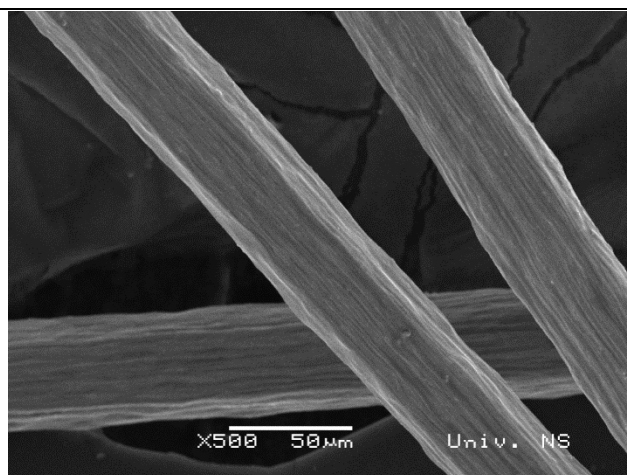


Figure 5. SEM micrograph of SS40 fibres (scale bar = 50 μm)

Diameters with SD of investigated fibre materials are presented in Table 2 showing that most of the applied fibre diameters are in the range from 12 to 44 μm. It should be noted that fibre diameters for fibres of rectangular or irregular cross-sections were approximated as circles with the same area. The exceptions are PPDJ and SSM fibres, which have much larger characteristic dimensions. As it was mentioned previously, PPDJ and SSM fibres have a rectangular cross-section, they look like wide strips, and therefore, they are defined by two characteristic lengths (Table 2). PPDJ fibres are significantly wider than SSM fibres as seen at optical micrographs of these fibres (Fig. 6).

Table 2. Fibre diameters/characteristic dimensions of investigated materials

Material	Fibre diameter ± SD, μm
Polyurethane (PU)	40 ± 4
Polypropylene (PP)	38 ± 3
Polypropylene bag (PPDJ)	1001 ± 14; 20 ± 4
Polyethylene terephthalate (BA1)	31 ± 2
Polyethylene terephthalate (PE)	38 ± 2
Stainless steel (SS40)	40 ± 2
Stainless steel (SS20)	20 ± 2
Stainless steel (SS12)	12 ± 0.8
Stainless steel sponge (SSM)	452 ± 11; 21 ± 3

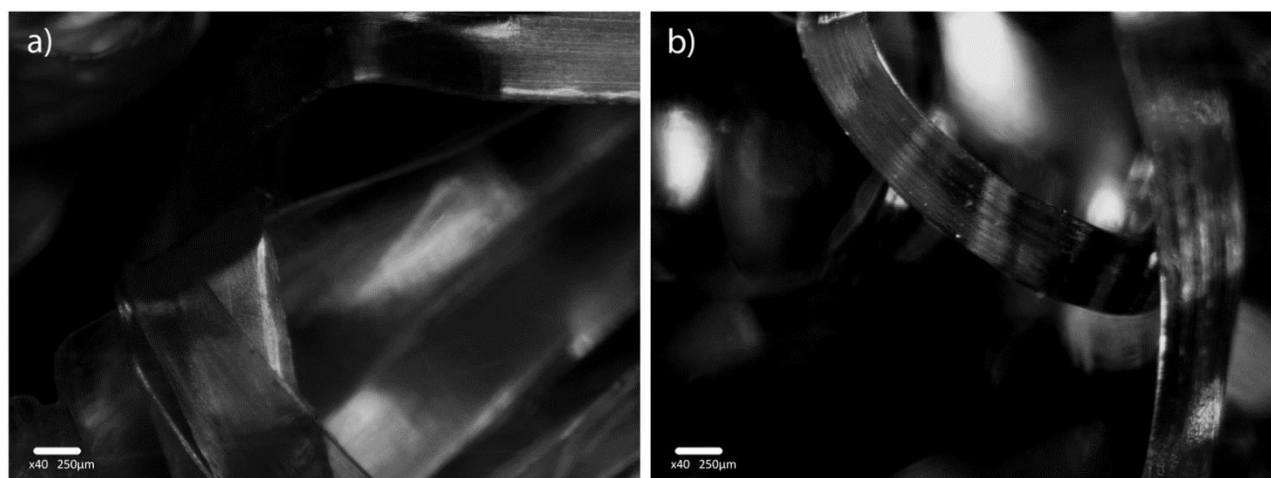


Figure 6. Optical micrographs of a) PPDJ fibres, b) SSM fibres (scale bar = 250 μm)

Visual appearance of packed fibres in filter beds with the same permeability and porosity was studied by optical microscopy. Figure 7. presents an overview of the SS40 fibre bed for permeability of $5.389 \times 10^{-9} \text{ m}^2$, marked as K_{01} . Two images that are presented in this figure are taken from different angles in the fibre bed under the same conditions. It could be seen that the pores are larger in Figure 7a, than those in Figure 7b, where the fibre packing is denser. Thus, it could be concluded that the SS40 fibre material forms two different regions in the filter bed regarding the porosity and pore size due to the material rigidity.

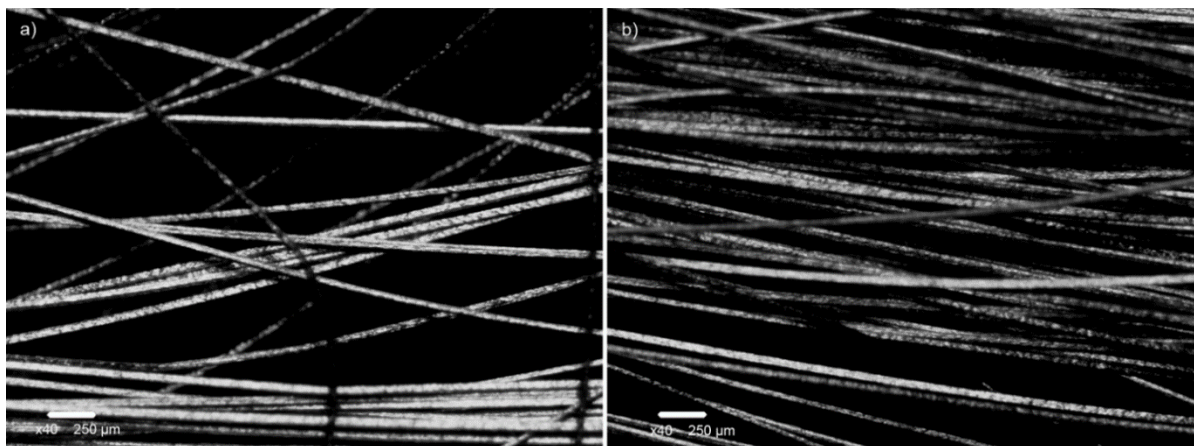


Figure 7. Optical micrographs of SS40 fibres at bed permeability K_{01} : a) region 1, b) region 2; (scale bar = 250 μm)

On the contrary, the stainless steel SS12 fibre bed at K_{01} permeability apparently has uniform pore distribution (Fig. 8). The SS12 fibres have much smaller diameters of $12 \pm 0.8 \mu\text{m}$, resulting in less rigid fibres than SS40 fibres. Therefore, the SS12 fibre bed consists of only one region, in which small and larger pores are mixed.

Figures 7 and 8 indicate that SS fibres, which differ in diameters, pack differently in the filter bed. It could be thus assumed that the diameter of stainless-steel fibres could affect their flexibility, which would directly affect fibre packing in the bed.

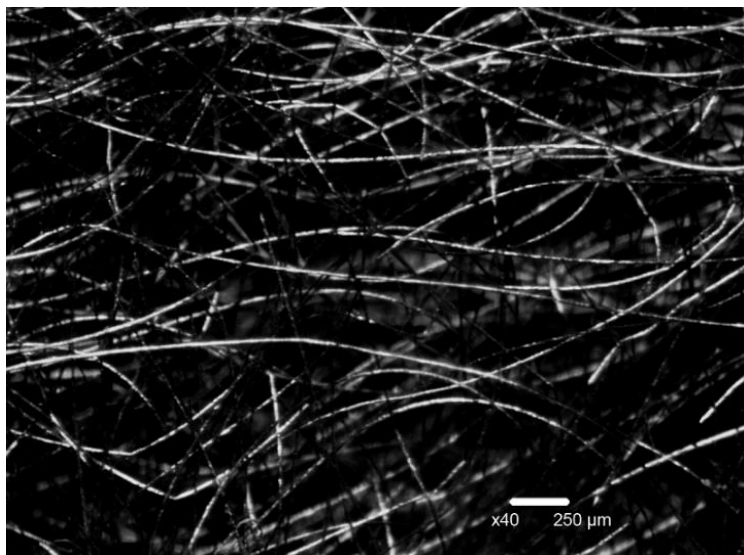


Figure 8. Optical micrograph of SS12 fibres at the permeability of K_{01} (scale bar = 250 μm)

All other investigated materials, especially polymer materials show similar pore distribution in filter bed as the SS12 filter bed (Fig. 9.)

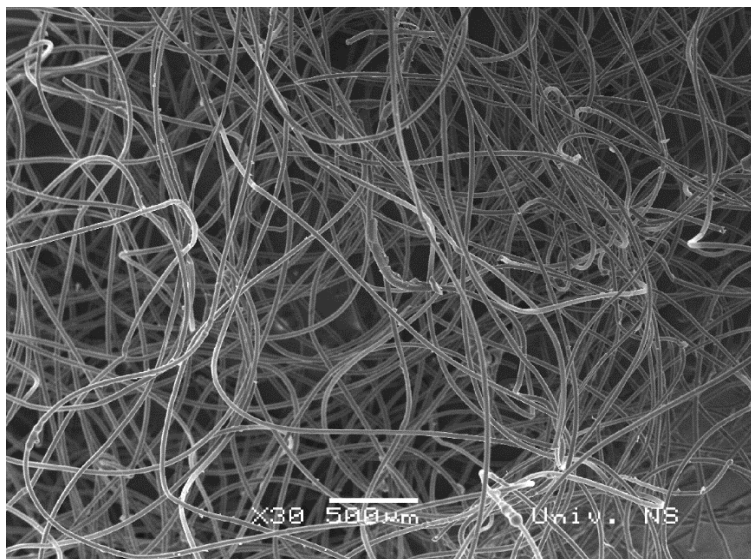


Figure 9. SEM micrograph of BA1 fibres (scale bar = 500 μm)

It should be noted that some of the investigated fibres are interconnected, such as PU fibres that form a sponge-like structure with pores in the honeycomb shape (Fig. 3). On the other hand, the PE material is composed of individual fibres that are connected at some points (Fig. 10).

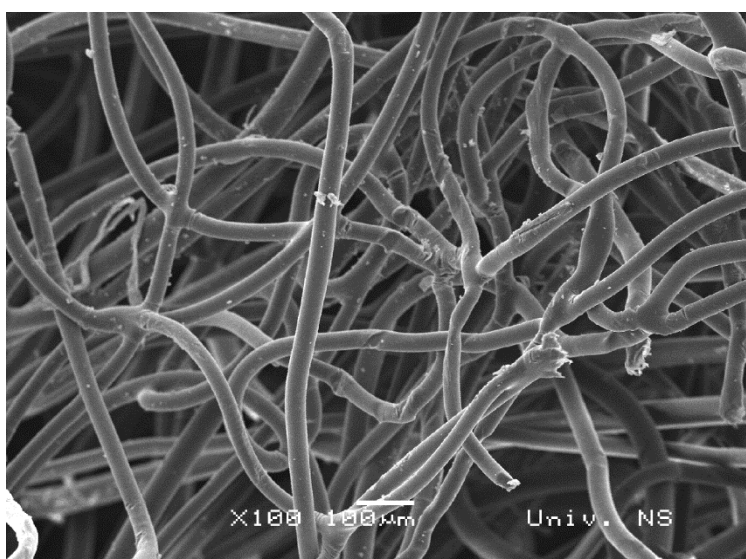


Figure 10. SEM micrograph of PE fibres (scale bar = 100 μm)

3. 2. The effect of fibre morphology on bed properties

In the previous section is seen, how different morphology influences packed bed appearance. However, the question remains whether and how these differences in the shape and dimensions of fibres reflect on the bed properties.

The investigation was conducted to define bed permeability using the Darcy's experiment for all fibre materials over different bulk densities, *i.e.* porosities. The dependence of the pressure drop per unit of bed length was linear for the entire range of investigated fluid velocities at all applied bed porosities ($R^2 \geq 0.990$). The Reynolds number was in the range from 0.01 to 0.38. The permeability values were then calculated based on the obtained slopes of the Darcy law, Eq. (2) [30]:

$$q = \frac{-kA\Delta p}{\mu L} \quad (2)$$

The pressure drop, Δp , was measured by piezometers, therefore Eq. (2) was rearranged, see Eq. (3):

$$\frac{\Delta h}{L} = \frac{b'}{\rho g} v = bv \tag{3}$$

This dependence for the PU fibre material is presented in Figure 11.

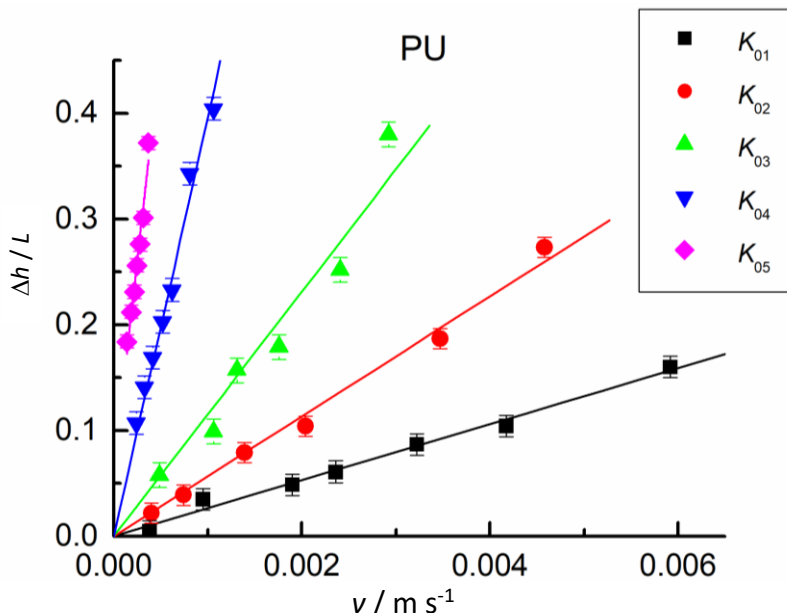


Figure 11. Experimental data and the best linear fits of height of water column per unit of the bed length ($\Delta h / L$) dependence on the fluid velocity (v) for PU fibre beds of different permeabilities

The obtained equations for PU filter beds and calculated values of bed permeabilities are presented in Table 3.

Table 3. The equations and R^2 values for PU fibre beds of different permeabilities

K / m^2	Equations	R^2
$5.38 \cdot 10^{-9} (K_{01})$	$\Delta h / L = 26.38 \pm 0.17 v$	0.990
$2.23 \cdot 10^{-9} (K_{02})$	$\Delta h / L = 58.60 \pm 0.31 v$	0.992
$1.13 \cdot 10^{-9} (K_{03})$	$\Delta h / L = 125.98 \pm 0.54 v$	0.991
$0.38 \cdot 10^{-9} (K_{04})$	$\Delta h / L = 374.23 \pm 1.88 v$	0.993
$0.18 \cdot 10^{-9} (K_{05})$	$\Delta h / L = 791.64 \pm 3.31 v$	0.991

*Numbers in the equation represent slope of the line, $b / s m^{-1}$

Based on bed permeabilities obtained by the Darcy experiment for defined porosities, the experimental dependence of bed porosity and bed permeability for all investigated materials can be established as presented in Figure 12. This is a very beneficial result because it allows formation of a fibre bed with desired bed permeability.

It should be noted that the behaviour of all tested materials except PPDJ, fits to the same experimental curve, Eq. (4) ($R^2 = 0.9547$), regardless of the studied properties of their fibres:

$$\varepsilon = 0.0366 \ln K_0 + 0.9124 \tag{4}$$

The flexibility of these fibres, their way of packaging, the connection of fibres, and their cross-section, for the investigated range, practically, do not affect the experimental dependence of porosity on permeability.

In Figure 12. it could be seen that the filter bed made of PPDJ fibres has a lower bed porosity for chosen bed permeability compared to the other investigated materials, Eq. (5). The equation for the PPDJ material ($R^2 = 0.9869$) is:

$$\varepsilon = 0.0393 \ln K_0 + 0.8534 \tag{5}$$

The complete set of data for PPDJ fibre beds is given in Table 4.



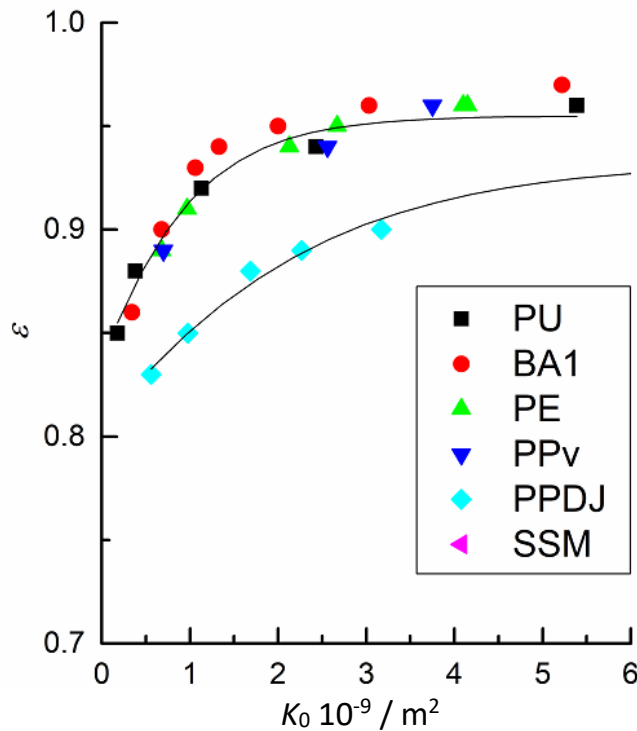


Figure 12. Experimental dependences of the bed porosity on the bed permeability for investigated materials

Table 4. Experimentally determined permeability values at different bed porosities for the PPDJ material

$K_0 10^{-9} / \text{m}^2$	ε
11.804	0.944
10.704	0.922
5.204	0.900
3.259	0.889
2.417	0.878
1.409	0.856
0.809	0.833

It is necessary to point out that from all investigated materials, fibres of polypropylene bags, PPDJ, have the largest dimensions. This fact can be the reason why the filter bed made of the PPDJ material has different dependence of the bed permeability on the bed porosity. Based on this result it could be concluded that the size of the fibre, has a much greater influence on bed properties than the shape of the fibre cross-section.

However, it should not be forgotten that SSM fibres are also much larger as compared to the other fibres, but still fit to the same experimental equation (4) as the other investigated materials apart from PPDJ.

4. CONCLUSION

In the investigation carried out, the studied PE, BA1, PP, and most SS fibres have circular cross-sections, the PU fibres have irregular cross-sections, while PPDJ and SSM fibres have rectangular cross-sections, which look like wide strips. The dimensions of fibres are in the range from 12 μm to 44 μm , except these of SSM and PPDJ fibres that are much larger.

The experimental dependence of the bed porosity on bed permeability was established where all investigated fibre materials yielded the same experimental equation, except for the PPDJ material, which yielded lower porosities at same permeabilities resulting in another functional dependence. The PPDJ fibres obtained from polypropylene bags have the largest dimensions, which could be the reason for the obtained differences. For all other investigated materials, the

fibre flexibility, way of packaging, the connection of fibres, and fibre cross-section, for the investigated range, practically, do not affect the experimental dependence of porosity on permeability.

The obtained experimental dependence of bed porosity on bed permeability could be used to form a bed in coalescer with predetermined, *i.e.* desired bed permeability. In this way, the bed geometry could be fixed, while the other parameters could be varied and investigated since the unknown and/or not defined bed geometry is the most common deficiency in the published literature dealing with bed coalescers, which often leads to contradictory conclusions.

NOMENCLATURE

ε	- porosity
$\rho_B / \text{kg m}^{-3}$	- bulk density
$\rho / \text{kg m}^{-3}$	- density of material
$\mu / \text{Pa}\cdot\text{s}$	- dynamic viscosity
$Q / \text{m}^3 \text{ s}^{-1}$	- volume flow
K / m^2	- bed permeability
A / m^2	- cross-section of filter bed
$\Delta p / \text{Pa}$	- pressure drop
$\Delta h / \text{cm H}_2\text{O}$	- height of water column
L / cm	- length of filter bed
$b', b / \text{s m}^{-1}$	- the slope of the line
$v / \text{m s}^{-1}$	- fluid velocity

Acknowledgements: The Ministry of Education, Science and Technological Development of the Republic of Serbia, Grant No. 172022, Grant No. 451-03-9/2021-14/200156, and Grant No. 451-03-9/2021-14/200134 supported the work.

We sincerely thank CEEPUS - Central European Exchange Program for University Studies for supporting the joint research by supporting the mobilities between the University of Novi Sad and TU Wien within the network "CIII-SI-0708-08-Chemistry and Chemical Engineering".

REFERENCES

- [1] Spielman LA. Separation of Finely Dispersed Liquid-Liquid Suspensions by Flow through Fibrous Media. Doctoral thesis, University of California, Berkeley, United States; 1968.
- [2] Spielman LA, Goren SL. Theory of Coalescence by Flow through Porous Media. *Ind Eng Chem Fundam.* 1972; 11 (1): 66-72. <https://doi.org/10.1021/i160041a011>
- [3] Spielman LA, Goren SL. Experiments in Coalescence by Flow through Fibrous Mats. *Ind Eng Chem Fundam.* 1972; 11 (1): 73-83. <https://doi.org/10.1021/i160041a012>
- [4] Amrei MM, Venkateshan DG, D'Souza N, Atulasimha J, Tafreshi HV. Novel Approach to Measuring the Droplet Detachment Force from Fibers. *Langmuir.* 2016; 32 (50): 13333-13339. <https://doi.org/10.1021/acs.langmuir.6b03198>
- [5] Bhattad P, Willson CS, Thompson KE. Effect of network structure on characterization and flow modeling using X-ray microtomography images of granular and fibrous porous media. *Transp Porous Media.* 2011; 90 (2): 363-391. <https://doi.org/10.1007/s11242-011-9789-7>
- [6] Bradford SA, Torkzaban S. Colloid interaction energies for physically and chemically heterogeneous porous media. *Langmuir.* 2013; 29 (11): 3668-3676. <https://doi.org/10.1021/la400229f>
- [7] Dawar S, Chase GG. Correlations for transverse motion of liquid drops on fibers. *Sep Purif Technol.* 2010; 72 (3): 282-287. <https://doi.org/10.1016/j.seppur.2010.02.018>
- [8] Elimelech M, Chen JY, Kuznar ZA. Particle Deposition onto Solid Surfaces with Micropatterned Charge Heterogeneity: The "Hydrodynamic Bump" Effect. *Langmuir.* 2003; 19 (17): 6594-6597. <https://doi.org/10.1021/la034516j>
- [9] Sokolović D, Govedarica D, Šećerov-Sokolović RM. Review: Influence of fluid properties and solid surface energy on efficiency of bed coalescence. *Chem Ind Chem Eng Q.* 2018; 24 (3): 210-230. <https://doi.org/10.2298/CICEQ170304034S>
- [10] Shou D, Fan J, Zhang H, Qian X, Ye L. Filtration Efficiency of Non-Uniform Fibrous Filters. *Aerosol Sci Technol.* 2015; 49 (10): 912-919. <https://doi.org/10.1080/02786826.2015.1083092>
- [11] Zhu P, Kong T, Tian Y, Tang X, Tian X, Wang L. Superwettability with antithetic states: Fluid repellency in immiscible liquids. *Mater Horiz.* 2018; 5 (6): 1156-1165. DOI: 10.1039/c8mh00964c

- [12] Herminghaus S. Roughness-induced non-wetting. *Europhys Lett.* 2000; 52 (2): 165-170. <https://doi.org/10.1209/epl/i2000-00418-8>
- [13] Miwa M, Nakajima A, Fujishima A, Hashimoto K, Watanabe T. Effects of the surface roughness on sliding angles of water droplets on superhydrophobic surfaces. *Langmuir* 2000; 16 (13): 5754-5760. <https://doi.org/10.1021/la991660o>
- [14] Xia F, Jiang L. Bio-inspired, smart, multiscale interfacial materials. *Adv Mater.* 2008; 20 (15): 2842-2858. <https://doi.org/10.1002/adma.200800836>
- [15] Zhang P, Wang S, Wang S, Jiang L. Superwetting surfaces under different media: Effects of surface topography on wettability. *Small.* 2015; 11 (16): 1939-1946. <https://doi.org/10.1002/smll.201401869>
- [16] Yohe ST, Freedman JD, Falde EJ, Colson YL, Grinstaff MW. A Mechanistic Study of Wetting Superhydrophobic Porous 3D Meshes. *Adv Funct Mater.* 2013; 23 (29): 3628-3637. <https://doi.org/10.1002/adfm.201203111>
- [17] Viswanadam G, Chase GG. Contact angles of drops on curved superhydrophobic surfaces. *J Colloid Interface Sci.* 2012; 367: 472-477. <https://doi.org/10.1016/j.jcis.2011.11.004>
- [18] Davoudi M, Fang J, Chase GG. Barrel shaped droplet movement at junctions of perpendicular fibers with different orientations to the air flow direction. *Sep Purif Technol.* 2016; 162: 1-5. <https://doi.org/10.1016/j.seppur.2016.02.009>
- [19] Šećerov Sokolović RM, Vulić TJ, Sokolović SM, Marinković-Nedučin RP. Effect of fibrous bed permeability on steady-state coalescence. *Ind Eng Chem Res.* 2003; 42 (13): 3098-3102. <https://doi.org/10.1021/ie020361i>
- [20] Šećerov Sokolović R, Stanimirović O, Sokolović S. The influence of fibrous bed bulk density on the bed properties. *Hem Ind.* 2003; 57 (7-8): 335-340. (in Serbian) <https://doi.org/10.2298/HEMIND0308335S>
- [21] Agarwal S, von Arnim V, Stegmaier T, Planck H, Agarwal A. Role of surface wettability and roughness in emulsion separation. *Sep Purif Technol.* 2013; 107: 19-25. <https://doi.org/10.1016/j.seppur.2013.01.001>
- [22] Agarwal S, von Arnim V, Stegmaier T, Planck H, Agarwal A. Effect of Fibrous Coalescer geometry and operating conditions on emulsion separation. *Ind Eng Chem Res.* 2013; 52 (36): 13164-13170. <https://doi.org/10.1021/ie4018995>
- [23] Fahim M, Othman F. Coalescence of secondary dispersions in composite packed beds. *J Dispers Sci Technol.* 1987; 8 (5-6): 507-523. <https://doi.org/10.1080/01932698708943620>
- [24] Das D, Ishtiaque SM, Das S. Influence of fibre cross-sectional shape on air permeability of nonwovens. *Fiber Polym.* 2015. 16 (1) 79-85. <https://doi.org/10.1007/s12221-015-0079-9>
- [25] Šećerov Sokolović RM, Govedarica DD, Sokolović DS. Selection of filter media for steady-state bed coalescers. *Ind Eng Chem Res.* 2014; 53 (6): 2484-2490. <https://doi.org/10.1021/ie404013e>
- [26] Kiralj A, Vulić T, Sokolović D, Šećerov Sokolović R, Dugić P. Separation of oil drops from water using stainless steel fiber bed. *Chem Ind Chem Eng Q.* 2017; 23 (2): 269-277. <https://doi.org/10.2298/CICEQ160610041K>
- [27] Govedarica DD, Šećerov-Sokolović RM, Kiralj AI, Govedarica OM, Sokolović DS, Hadnađev-Kostić MS. Separation of mineral oil droplets using polypropylene fibre bed coalescence, *Hem Ind.* 2015; 69 (4): 339-346. <https://doi.org/10.2298/HEMIND140322047G>
- [28] Srđan S. Sokolović, Arpad I. Kiralj, Dunja S. Sokolović, Aleksandar I. Jokić, Application of waste polypropylene bags as filter media in coalescers for oily water treatment, *Hem Ind.* 2019; 73 (3) 147-154 <https://doi.org/10.2298/HEMIND190311013S>
- [29] Das, D., Ishtiaque, S.M., Das, S. Influence of fibre cross-sectional shape on air permeability of nonwovens. *Fiber Polym.* 2015; 16: 79-85. <https://doi.org/10.1007/s12221-015-0079-9>
- [30] Cerepi A., Burlot R., Galaup S., Barde J. -P., Loisy C., Humbert L., Effects of porous solid structures on the electrical behaviour: prediction key of transport properties in sedimentary reservoir rock, *Stud Surf Sci Cat.* 2002;144: 483-490. [https://doi.org/10.1016/S0167-2991\(02\)80171-9](https://doi.org/10.1016/S0167-2991(02)80171-9)

Uticaj morfologije vlakana na fenomen pakovanja i svojstva sloja u koalescerima

Milica Hadnađev Kostić¹, Dunja Sokolović², Srđan Sokolović³, Thomas Laminger^{4, 5} i Arpad Kiralj¹

¹Univerzitet u Novom Sadu, Tehnološki fakultet, Bul. Cara Lazara 1, Novi Sad, Srbija

²Univerzitet u Novom Sadu, Fakultet tehničkih nauka, Trg Dositeja Obradovića 6, Novi Sad, Srbija

³NIS a.d. Novi Sad, Srbija, Narodnog fronta 12, Novi Sad, Srbija

⁴Tehnički Univerzitet u Beču, Institut za hemijsko inženjerstvo, Austrija TU WIEN, Getreidemarkt 9/166, A-1060 Beč, Austrija

⁵AGRANA Stärke GmbH - Werk Pischelsdorf, Industriegelände, 3435 Pischelsdorf, Austrija

(Stručni rad)

Izvod

U ovom radu ispitivana je morfologija vlakana otpadnih materijala i njihov uticaj na fenomen pakovanja i svojstva filtracionog sloja u koalescerima. Ispitivano je devet otpadnih materijala. Skenirajućom elektronskom mikroskopijom utvrđeno je da su površine svih vlakana glatke, dok se poprečni presek razlikuje od kružnog, pravougaonog do nepravilnog. Vlakna kružnog poprečnog preseka imala su prečnike u opsegu od $12\pm 0,8$ do 40 ± 4 μm , dok su vlakna polipropilenskih vreća i vlakna sunđerastog nerđajućeg čelika bila trake, širine 452 ± 11 i 1001 ± 14 μm , redom. Takođe, je primećeno da su poliuretanska vlakna povezana formirajući sunđerastu strukturu, dok su vlakna polietilen tereftalata samo na nekim mestima međusobno povezana. U ovom radu ustanovljena je eksperimentalna zavisnost poroznosti sloja od permeabilnosti sloja za sve ispitivane materijale, što omogućava formiranje sloja vlakana željene permeabilnosti. Izuzetak je sloj formiran od vlakana polipropilenskih vreća koja su najvećih dimenzija tako da je ovaj sloj pokazao različitu zavisnost poroznosti od permeabilnosti sloja u odnosu na ostale ispitivane materijale.

Ključne reči: propustljivost sloja, poroznost sloja, sloj vlakana, koalescentna filtracija